small NANO MICRO

Drug delivery

Sustained Drug Release from Non-eroding Nanoporous Templates**

*Evin Gultepe, Dattatri Nagesha, Bernard D. F. Casse, Ravinder Banyal, Trifon Fitchorov, Alain Karma, Mansoor Amiji, and Srinivas Sridhar**

Mechanically robust implants are being used in many different parts of the body for various applications in orthopedics, cardiovascular stents, and defibrillators.[1,2] However, there are numerous problems to overcome, such as reducing infections, enhancing implant bonding, and preventing restenosis in cardiovascular stents, among others. A central strategy is to incorporate therapeutic agents that can enhance implants and overcome the key problems mentioned.[3–5] A popular approach is to incorporate polymer coatings that are loaded with the therapeutic agent.[6,7] However, in some cases polymers are not the most suitable materials, such as in cardiovascular stents where delamination of the polymer coating can lead to thrombosis.[8,9] In those situations it is necessary to have a reservoir that does not degrade or erode. Non-eroding nanoporous oxide coatings offer an attractive alternative platform since they are nonerodible and their nanofeatures allow control of the elution profile.

Herein, we present the results for the release of a model drug, doxorubicin (Dox), from different non-eroding nanoporous coatings. Detailed studies of drug release from these platforms in the form of anodic aluminum oxide (AAO) and anodic titanium oxide (ATO) were carried out. There are many approaches to sputter metals, such as titanium and aluminum, on different materials and to anodize them afterwards,[10,11] thus giving feasibility to the integration of the nanoporous templates on implants or stents. We show that nanoporous surfaces can achieve a sustained release rate over periods of several weeks, similar to polymeric platforms but without the risk of delamination or leaching since they are not degradable. We show that the kinetics of the sustained release from these nanoporous platforms is well described by an activated surface-density-dependent desorption model, which appears to be universal for non-eroding platforms.

The release studies were performed in vitro using phosphate-buffered saline (PBS), which is commonly employed to simulate in vivo conditions for drug release.[12,13] The elution kinetics is fundamentally the same in vivo since the nanoporous platforms are not affected by the physiological conditions, unlike their polymeric or hydrogel counterparts. Besides, in the case of small molecules such as Dox, enzymes would not interfere with the drug and hence the elution kinetics is not altered by the presence of the biomolecules. In this study, the results prove that the nanoporous platforms can be used as non-eroding sustained-release systems that can be utilized as coatings on currently available implants, such as cardiovascular stents, orthopedic/dental implants, fiducial implants, or spacers.

The biocompatibility of titanium, aluminum, and their oxides has already been well established and they have been used widely in orthopedic prostheses and dental implants for years.[14–18] Some studies of nanoporous coatings of alumina for drug-release applications have been carried out before.[10,19–21] ATO nanotubes, although a relatively new material compared to AAO, have also been investigated as drug-release platforms in the past.[22,23] Studies have shown that titania-nanotube coatings are not only biocompatible but also support bone growth.[24–26] Although drug release from nanoporous coatings has been studied before, there is a lack of understanding of the release kinetics from these platforms and the dynamics governing them. Herein, our aim is to explain the release kinetics from nanoporous surfaces by a model that is supported with a systematic study of elution profiles.

Three different types of platforms were used for the elution studies: AAO nanotemplates (Figure 1a and b), ATO nanotemplates (Figure 1c), and a biodegradable polycaprolactone (PCL) as control platform. Dox, which is a self-fluorescent drug, was loaded into the templates for the release studies.

A custom-made fluorometry setup (Figure 2) was built to enable in situ measurements, that is, the fluorescence intensity of Dox was measured directly inside the release medium. This in situ measurement method made it possible to achieve a large

[*] Prof. S. Sridhar, E. Gultepe, Dr. D. Nagesha, Dr. B. D. F. Casse, Dr. R. Banyal
Electronics Materials Research Institute and Department of Physics
Northeastern University
Boston, MA 02115 (USA)
E-mail: s.sridhar@neu.edu

T. Fitchorov
Department of Electrical and Computer Engineering and
Center for Microwave Magnetic Materials and Integrated Circuits
Northeastern University
Boston, MA 02115 (USA)

Prof. A. Karma
Department of Physics
Northeastern University
Boston, MA 02115 (USA)

Prof. M. Amiji
Department of Pharmaceutical Sciences
Northeastern University
Boston, MA 02115 (USA)

[**] The authors gratefully acknowledge the helpful suggestions of Prof. Clive Perry. This study was funded by the IGERT Nanomedicine Science and Technology Program (NSF-0504331).

Supporting Information is available on the WWW under http://www.small-journal.com or from the author.

DOI: 10.1002/smll.200901736

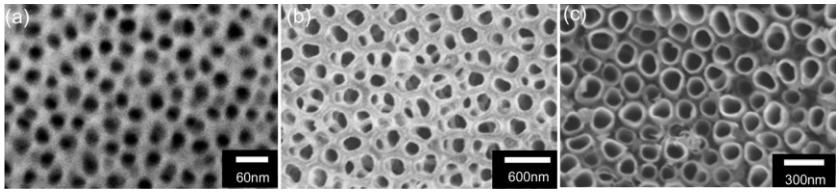

Figure 1. Scanning electron microscopy images of non-eroding nanoporous templates. a) AAO, 20 nm pore diameter (AAO-20); b) AAO, 200 nm pore diameter (AAO-200); c) ATO, 125 nm pore diameter.

number of readings without disturbing the release process. This design is critical to understand the release kinetics, since it allows the collection of fast and frequent data over time.

All the platforms showed release profiles extending to the order of weeks and were still eluting when the measurements were terminated. Figure 3 shows representative graphs of the percentage of drug released from different platforms. The percent release was calculated by comparing the drug released into the medium to the total drug released at infinite time (M_∞). For nanotemplates M_∞ was estimated by clearing the drug completely from the pores with the help of an emulsifier, Tween 80, after the elution measurements (see the Supporting Information for the protocol diagram, Figure S3). The drug released at infinite time is the sum of the amount of drug in the Tween solution (M_T) and the total drug eluted during the experiments (M): $M_\infty = M + M_T$. For polymeric platforms, on the other hand, M_∞ is known exactly by the preparation method.

All the platforms show a considerable amount of drug release immediately after introduction to the release medium — this effect is known as the burst release. The time period for the burst release is relatively very short compared to the entire release process and is typically about 100 min for the platforms investigated. Although burst release has been observed in many controlled-release studies, due to the short time range there are few detailed data in this region and it has been ignored in most of the mathematical models.[27]

One of the advantages of the in situ measurement setup used in these experiments is that it is possible to collect release data frequently, at minute intervals, which helps in understanding the short-term burst effect. The burst-release data for the first 100 min fit to the same power law behavior for all non-eroding and polymeric platforms: $m(t)/M_\infty = y_0 + at^{1/2}$, where $m(t)$ is the cumulative released drug, and y_0 and a are the fitting parameters (Figure 4a). The release rate ($dm(t)/dt$) of such a system is inversely proportional to the square root of the time: $dm/dt = \kappa t^{-1/2}$, where the rate constant $\kappa = \frac{1}{2} M_\infty a$. The $t^{1/2}$ dependence is characteristic of Fickian diffusion, considering that in this early stage the drug is diffusing into a semi-infinite medium with zero initial concentration.[28]

After the burst-release phase, all the platforms start releasing the drug at a much slower rate. The non-eroding nanoporous coatings show an empirical logarithmic behavior (Figure 4b): $m(t)/M_\infty = \ln(b + ct)$, where b and c are fitting parameters. The empirical constant c in the release equation depends on the effective surface area of the template, which is quite magnified due to one of the advantages of the nanofeatures of the platform, namely the enhanced surface-to-volume ratio (Figure 5a; see the Supporting Information for details). This dependency suggests that the sustained release is not dominated mainly by the diffusion, but by the drug–surface interactions, that is, surface desorption. The release profile also suggests a density-activated release model: the fewer the number of drug molecules left on the surface, the faster the release rate (Figure 5b). Hence, the release profile is determined not only by the interaction between drug molecules and the surface, but also by the interaction between the drug molecules.

The experimental results can be interpreted with a desorption model, which assumes that the time rate of change of the fractional surface coverage f obeys the simple first-order kinetic law $\frac{df}{dt} = k(t)f^n$, where k is the rate of desorption of particles from the surface.[29] Since desorption is a thermally activated process, the rate constant obeys an Arrhenius law $k(t) = k\exp(-E_a(t)/k_B T)$, in which k_B is the Boltzmann constant.[30] The activation energy E_a, and hence the desorption rate, generally depends on surface coverage,[31] thus reflecting the fact that this energy is determined by both the interaction of particles with the substrate and the interaction between particles. The latter becomes relevant for large surface coverage when the mean distance between particles becomes comparable to the particle radius. Since the probability for two particles to interact is proportional to f^2, the activation energy

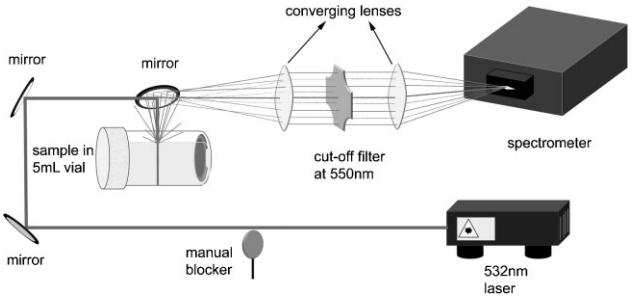

Figure 2. Experimental setup for in situ fluorescence measurements.

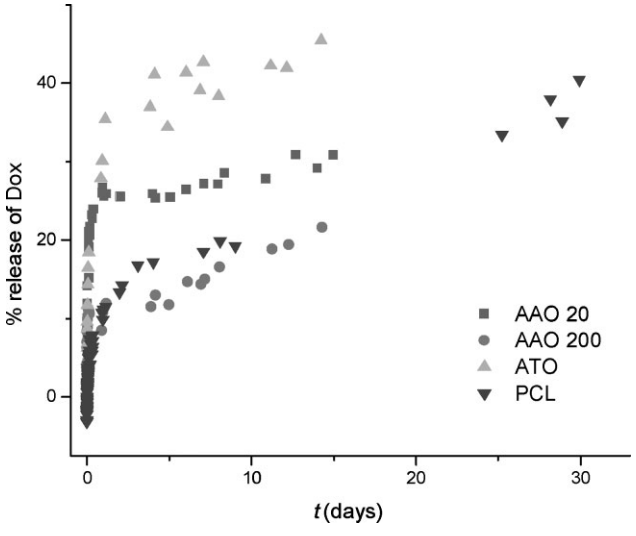

Figure 3. Representative curves for the percentage of Dox released from each platform.

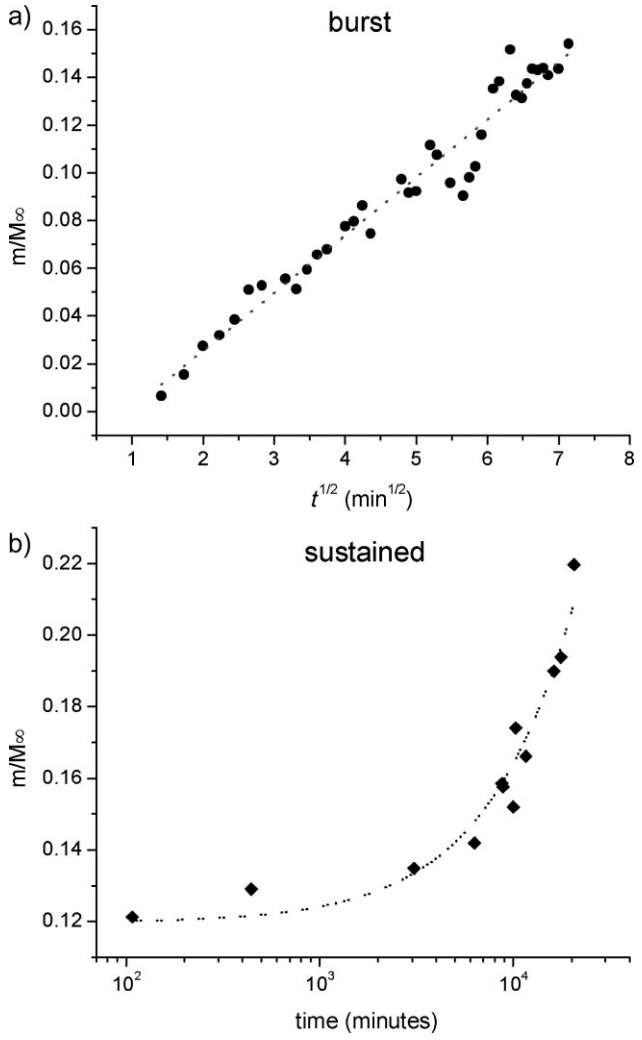

Figure 4. a) Representative graph of the initial release profile fitted to $m(t)/M_\infty = y_0 + at^{1/2}$. b) Representative slow-release profile for non-eroding platforms fitted to $m(t)/M_\infty = \ln(b + ct)$. The x axis is on a log scale.

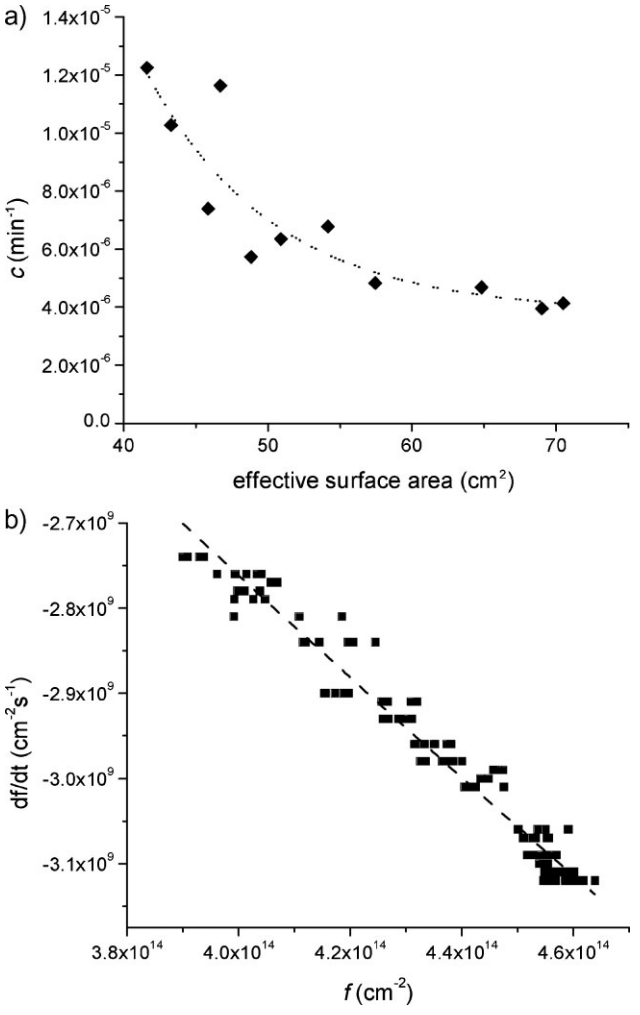

Figure 5. a) Change of parameter c in the release equation, $m(t)/M_\infty = \ln(b + ct)$, as a function of effective template surface area. b) Representative graph of the change in the number of particles over the surface, which depends on the coverage itself. The line is the fitting of the data to the surface desorption model, $df/dt = -\alpha f \exp(-\beta f^2/k_B T)$.

can be written in the mean-field limit as $E_a = E_a^0 + \beta f^2$, where E_a^0 represents the interaction of the particle with the substrate and βf^2 is the increase of the activation energy due to the pairwise particle interactions. This yields the prediction $df/dt = -\alpha f \exp(-\beta f^2/k_B T)$, where the vanishing-coverage-limit rate constant is defined as $\alpha = \exp\left(-\frac{E_a^0}{k_B T}\right)$.

The above theoretical prediction is seen to fit well for the data from all of the nanoplatforms. The absolute coverage rate decreases with declining coverage; Figure 5b shows a representative curve fitting. The fitting parameters for each non-eroding platform are summarized in Table 1.

We carried out drug-release studies from PCL plugs as a comparison platform. PCL plugs showed same burst-release behavior of $t^{1/2}$ dependency as the non-eroding ones. However, their profile was different from that of the non-eroding platforms for slow release. It shows a power law similar to burst release but with a different exponent: $m(t)/M_\infty = kt^n$ (data not shown), where k is the fitting parameter and the exponent $n = 0.31 \pm 0.01$, which is consistent with the elution kinetics of polymeric platforms in the literature.[32–34]

Table 1. Fitting parameters of release data to the surface desorption model, $df/dt = -\alpha f \exp(-\beta f^2/k_B T)$.

Platform	$\alpha \times 10^{-6}$ [s^{-1}]	$\beta \times 10^{-47}$ [J m^2]
AAO-20	-6 ± 1	-8 ± 5
AAO-200	-7 ± 1	-4 ± 2
ATO	-17 ± 0.6	-27 ± 10

In summary, we have shown that biocompatible, non-eroding nanoporous coatings can be fabricated that are suitable for drug-releasing implants for a variety of therapeutic situations. Nanoporous platforms were loaded with Dox and the release profile was observed by in situ fluorometry. After a rapid burst release, which was similar for all the platform types, different sustained-release kinetics was observed from the nanoporous platforms. An activated surface-density-dependent desorption was in effect for nanoporous templates. The results provide direct evidence that nonerodible, biocompatible nanoporous coatings can be manufactured that are suitable for sustained drug release from implants for a variety of therapeutic situations as alternatives to polymeric systems.

Experimental Section

Platform fabrication: Three types of non-eroding and one type of polymeric platform were prepared for the study, namely AAO with pore sizes of 20 (AAO-20) and 200 nm (AAO-200), ATO, and PCL. Nanoporous alumina templates were prepared by anodization of aluminum foil in an acid;[35] the anodization setup is shown in Figure S1 (Supporting Information). AAO-20 platforms were prepared by two-step anodization[36] of aluminum foil (Alfa Aesar) under a constant voltage of 15 V in oxalic acid solution (5 wt%). The second step was carried out for 4 h resulting in a 20 nm pore diameter and 2 μm array thickness. AAO-200 platforms were also prepared by the same two-step anodization method but at 130 V and in phosphoric acid solution (0.3 M). Following 4 h of second-step anodization, the platforms were immersed in phosphoric acid (5%) for 80 min for pore widening. Then, an AAO of pore diameter 200 nm and array thickness 10 μm was achieved. ATO platforms were fabricated by anodization of titanium foil (Alfa Aesar) under a constant voltage of 60 V and in potassium fluoride (0.05M in 10% deionized (DI) water/90% glycerol) solution. After 15 h of anodization, nanotubes 125 nm in diameter and 2.5 μm in length were achieved as reported in the literature.[37] The templates were soaked in Dox (adriamycin, 2 mg mL^{-1})/PBS (500 μL, 50 μg mL^{-1}) for 24 h. PCL–Dox platforms were prepared by mixing dissolved PCL and Dox. First, PCL (0.4 g) was dissolved in acetone (1 mL) to give a homogeneous solution. Dox (2 mg mL^{-1}, 20 vol%, 100 μL) was added to the PCL solution and mixed thoroughly. The liquid solution was placed in 500-μL-capacity microcentrifuge tubes and dried overnight. The dried PCL was removed from the centrifuge tubes and the resulting self-standing PCL cones were used as a representative polymeric drug-release platform. Images of the platforms after loading are shown in Figure S2 (Supporting Information).

In situ release profile measurement: The nanoporous templates were first washed with DI water (1 mL) to remove residues of Dox on the surface. All the release platforms (four replicas of AAO-20 and AAO-200, three replicas of ATO, and five replicas of PCL) were placed in glass scintillation vials with PBS (5 mL, 1%) buffer solution as the release medium. The fluorescence signal, which was directly proportional to the amount of Dox in the solution, was measured directly in the release medium using a custom-built spectrometer design (Figure 2). The laser beam at a wavelength of 532 nm was shone onto the vial at predetermined time intervals. The fluorescence emission of Dox at 590 nm was detected by the spectrometer (MS257 Oriel, CT). The acquisition time of the spectrometer was set at 0.5 s and to avoid bleaching of the Dox, the vials were kept under the laser no longer than necessary. Between measurements the vials were kept on a rocker to allow constant mixing of the solution. More details can be found in the Supporting Information.

Keywords:

drug delivery · fluorescence · nanoporous materials · surface desorption · sustained release

[1] W. Greatbatch, C. F. Holmes, *IEEE Eng. Med. Biol. Mag.* **1991**, *10*, 38.
[2] E. Regar, G. Sianos, P. W. Serruys, *Br. Med. Bull.* **2001**, *59*, 227.
[3] R. S. Schwartz, N. A. Chronos, R. Virmani, *J. Am. Coll. Cardiol.* **2004**, *44*, 1373.
[4] B. Peter, D. P. Pioletti, S. Laib, B. Bujoli, P. Pilet, P. Janvier, J. Guicheux, P. Y. Zambelli, J. M. Bouler, O. Gauthier, *Bone* **2005**, *36*, 52.
[5] D. P. Pioletti, O. Gauthier, V. A. Stadelmann, B. Bujoli, J. Guicheux, P. Y. Zambelli, J. M. Bouler, *Curr. Drug Delivery* **2008**, *5*, 59.
[6] A. Chieffo, A. Colombo, *Herz* **2004**, *29*, 147.
[7] J. S. Price, A. F. Tencer, D. M. Arm, G. A. Bohach, *J. Biomed. Mater. Res.* **1996**, *30*, 281.
[8] G. Maluenda, G. Lemesle, R. Waksman, *Clin. Pharmacol. Ther.* **2009**, *85*, 474.
[9] P. A. Gurbel, D. E. Kandzari, *Neth. Heart J.* **2007**, *15*, 148.
[10] H. Wieneke, O. Dirsch, T. Sawitowski, Y. L. Gu, H. Brauer, U. Dahmen, A. Fischer, S. Wnendt, R. Erbel, *Catheter Cardiovasc. Interv.* **2003**, *60*, 399.
[11] E. P. Briggs, A. R. Walpole, P. R. Wilshaw, M. Karlsson, E. Palsgard, *J. Mater. Sci. Mater. Med.* **2004**, *15*, 1021.
[12] R. Wessely, J. Hausleiter, C. Michaelis, B. Jaschke, M. Vogeser, S. Milz, B. Behnisch, T. Schratzenstaller, M. Renke-Gluszko, M. Stover, E. Wintermantel, A. Kastrati, A. Schomig, *Arterioscler. Thromb. Vasc. Biol.* **2005**, *25*, 748.
[13] S. V. Ranade, K. M. Miller, R. E. Richard, A. K. Chan, M. J. Allen, M. N. Helmus, *J. Biomed. Mater. Res. Part A* **2004**, *71A*, 625.
[14] E. Gultepe, D. Nagesha, S. Sridhar, M. Amiji, *Adv. Drug Delivery Rev.* DOI: 10.1016/j.addr.2009.11.003
[15] L. Sedel, *Clin. Orthop. Relat. Res.* **2000**, 48.
[16] M. Long, H. J. Rack, *Biomaterials* **1998**, *19*, 1621.
[17] M. N. Helmus, D. F. Gibbons, D. Cebon, *Toxicol. Pathol.* **2008**, *36*, 70.
[18] H. L. Freese, M. G. Volas, C. R. Wood, M. Textor, in *Encyclopedia of Materials: Science and Technology*, (Eds.: K. H. J. Buschow, R. Cahn, M. Flemings, B. Ilschner, E. J. Kramer, S. Mahajan, P. Veyssière), Informa Health Care, New York **2003**.
[19] K. E. La Flamme, G. Mor, D. Gong, T. La Tempa, V. A. Fusaro, C. A. Grimes, T. A. Desai, *Diabetes Technol. Ther.* **2005**, *7*, 684.
[20] R. Langer, J. P. Vacanti, *Science* **1993**, *260*, 920.
[21] D. Gong, V. Yadavalli, M. Paulose, M. Pishko, C. A. Grimes, *Biomed. Microdevices* **2003**, *5*, 75.
[22] K. C. Popat, M. Eltgroth, T. J. LaTempa, C. A. Grimes, T. A. Desai, *Biomaterials* **2007**, *28*, 4880.
[23] K. C. Popat, M. Eltgroth, T. J. LaTempa, C. A. Grimes, T. A. Desai, *Small* **2007**, *3*, 1878.
[24] C. Yao, V. Perla, J. L. McKenzie, E. B. Slamovich, T. J. Webster, *J. Biomed. Nanotechnol.* **2005**, *1*, 68.
[25] K. C. Popat, L. Leoni, C. A. Grimes, T. A. Desai, *Biomaterials* **2007**, *28*, 3188.
[26] B. D. Boyan, T. W. Hummert, D. D. Dean, Z. Schwartz, *Biomaterials* **1996**, *17*, 137.
[27] X. Huang, C. S. Brazel, *J. Controlled Release* **2001**, *73*, 121.
[28] J. Crank, *The Mathematics of Diffusion*, Oxford University Press, New York **1979**.
[29] K. Oura, V. G. Lifshits, A. A. Saranin, A. V. Zotov, M. Katayama, *Surface Science: An Introduction*, Springer, Berlin **2003**.
[30] P. A. Redhead, *Vacuum* **1962**, *12*, 203.
[31] J. T. Yates, in *Methods of Experimental Physics: Solid State Physics: Surfaces*, Vol. *22* (Eds: R. L. Park, M. G. Lagally), Academic Press, Orlando **1985**, p. 425.
[32] T. Higuchi, *J. Pharm. Sci.* **1963**, *52*, 1145.
[33] P. Ritger, N. Peppas, *J. Controlled Release* **1987**, *5*, 23.
[34] V. Lemaire, J. Belair, P. Hildgen, *In. t J. Pharm.* **2003**, *258*, 95.
[35] E. Gultepe, D. Nagesha, L. Menon, A. Busnaina, S. Sridhar, *Appl. Phys. Lett.* **2007**, *90*, 163119.
[36] H. Masuda, M. Satoh, *Jpn. J. Appl. Phys.* **1996**, *35*, L126.
[37] A. L. Friedman, E. Panaitescu, C. Richter, L. Menon, *J. Nanosci. Nanotechnol.* **2008**, *8*, 5864.

Received: September 15, 2009
Published online: December 4, 2009

